Usefulness of medium-Energy Collimator for Sentinel Node Lymphoscintigraphy Imaging in Breast Cancer Patients

Usefulness of Medium-Energy Collimator for Sentinel Node Lymphoscintigraphy Imaging in Breast Cancer Patients

Hiroyuki Tsushima, PhD[1,2], Teruhiko Takayama, MD[2], Takashi Yamanaga, RT[1], Hiroto Kizu, PhD[2], Yoshihiro Shimonishi, RT[1], Kazuhisa Kosakai, RT[1], Atsushi Noguchi, PhD[2], and Masahisa Onoguchi, PhD[2]

[1]Department of Radiological Technology, Osaka City University Hospital, Asahimachi, Abeno, Osaka, Japan; and [2]Department of Health Sciences, Graduate School of Medical Science, Kanazawa University, Kodatsuno, Kanazawa, Japan

This study was performed to investigate the usefulness of a general-purpose medium-energy (ME) collimator for the accurate localization of the sentinel lymph node (SLN) in breast cancer patients. **Methods:** We compared phantom images and lymphoscintigraphy images obtained under different conditions for a patient with breast cancer. Comparisons were performed between 2 cameras, between a low-energy high-resolution (LEHR) collimator and a general-purpose ME collimator, and between energy windows centered at 141 keV and at 146 keV. Profile curves and image contrast were evaluated along with the visual interpretation of images. The most suitable imaging time was selected from the relationship between contrast and the data acquisition time. **Results:** The images obtained with the general-purpose ME collimator and the energy window centered at 141 keV were of poorer quality than those obtained with the LEHR collimator and the same energy window. However, the quality of the images obtained with the general-purpose ME collimator improved when the energy window was centered at 146 keV. The method involving the general-purpose ME collimator and the energy window centered at 146 keV showed excellent image quality similar to that obtained with the LEHR collimator. The enhancement of contrast was confirmed at more than 3 cm away from the center of the injection site. Stable contrast was obtained with a data acquisition time of 5 min, with the general-purpose ME collimator, and with the energy window centered at 146 keV. **Conclusion:** The method involving the general-purpose ME collimator and the energy window centered at 146 keV has the merit of the lymph node not being concealed by a lead shield. This new method is expected to improve the rate of detection of SLN and has the potential for shortening the acquisition time.

Key Words: sentinel lymph node; breast cancer; lymphoscintigraphy; medium-energy collimator; star-shaped artifacts

J Nucl Med Technol 2006; 34:153–159

Since the introduction of the concept of radionuclide sentinel lymph node (SLN) identification in the management of melanoma, radionuclide sentinel node lymphoscintigraphy has rapidly become an accepted means of evaluating regional lymph node status for melanoma and breast tumors (*1–8*). The advantages of radionuclide lymphoscintigraphy over the blue dye method include ease of injection, shorter time interval between injections, and improved SLN detection (*9*). On the other hand, radionuclide lymphoscintigraphy has some disadvantages, particularly with breast node studies. The target tissues are small and contain only a small amount of radioactivity. A large amount of activity is retained at the injection site and can cause artifacts through scatter or septal penetration (*8*).

The technique for lymphatic mapping is well established for melanoma but not for breast cancer (*7*). Furthermore, technique is very important for minimizing artifacts and improving lesion detection during breast imaging (*10–17*). Placing a small lead shield over the injection site has been reported in the literature (*9*). However, the use of a lead shield has the disadvantage that the lead shield may conceal the SLN. To avoid the possibility of a lead shield concealing the SLN, we devised a new method using a medium-energy (ME) collimator without a lead shield. We also tried to adjust the center of the energy window because it was reported that adjustment of the energy window might at times assist in the imaging of lymph nodes that are close to the injection site (*1*). We developed an imaging phantom based on the clinical data and evaluated the usefulness of an ME collimator for the accurate localization of SLNs in breast cancer patients.

MATERIALS AND METHODS

Phantoms

To evaluate the usefulness of an ME collimator for sentinel node lymphoscintigraphy in breast cancer patients, we used 3 types of phantoms made of acrylic plates. The first phantom, an injection site phantom (IS phantom), was a cylindric source that was 2 cm in diameter and 1 cm thick and contained 40 MBq of

Received Jul. 5, 2005; revision accepted May 15, 2006.

For correspondence or reprints contact: Hiroyuki Tsushima, PhD, Department of Radiological Technology, Osaka City University Hospital, 1-5-7 Asahimachi, Abeno, Osaka 545-8586, Japan.

E-mail: tsushima@med.osaka-cu.ac.jp

^{99m}Tc-pertechnetate. The second phantom, a lymph node phantom (LN phantom), was made to estimate the effect of the concentration of radioactivity on image quality. The phantom was constructed of a 15 × 30 cm square plate that was 1 cm thick and had 30 holes (Figs. 1A and 1C). The 30 holes were divided into 3 groups of 10 holes with diameters of 6.0, 8.5, and 12 mm for groups 1, 2, and 3, respectively. The concentration of ^{99m}Tc-pertechnetate in 10 holes was changed from 0.78 to 400 kBq/200 μL in 1:2 increments over 10 steps so that the lymph node image density might vary stepwise in accordance with the concentration of radioactivity. The surface and the bottom of the acrylic plate were covered with waterproof sheets to prevent the leakage of radiopharmaceuticals. The third phantom, a combination phantom (CB phantom), simulating both injection site and SLNs, was used to study the effect of the distance from the injection site to the lymph node on image quality. A lymph node was simulated by 40 kBq of ^{99m}Tc-pertechnetate placed in a hole in a 2 × 2 cm square acrylic plate that was 1 cm thick. The measurements of the simulated lymph node were 5 and 10 mm. As shown in Figure 1B, a total of 12 plates with a hole were aligned 3, 5, and 7 cm from the center of the IS phantom in both the horizontal (H) direction and the oblique (S) direction; these directions were selected because they align with where one would expect to see star artifacts resulting from septal penetration. Figure 1D shows an illustration of this phantom.

Imaging

This study was performed with 2 dual-head γ-cameras: a FORTE (ADAC) and a DSX rectangular (Sopha Medical Corp.). Standard imaging was performed with a FORTE camera because that camera showed the best image quality. To study the effect of radioactivity in the lymph nodes on image quality, the LN phantom was imaged by use of the FORTE camera with a low-energy (LE) high-resolution (LEHR) collimator and the energy window centered at 141 keV (±5%) for 250 s of data acquisition. The image matrix was 256 × 256 (1 pixel = 2.36 mm).

To compare the performances of the 2 cameras attached to an LE collimator, the IS phantom was imaged. Before imaging, we made 2 assumptions. One is that the attenuation and the scattering of γ-rays caused by a patient's body are equal to the values for an acrylic plate that is 20 cm thick. The other is that the SLNs in breast cancer patients are located at a depth of 2 cm. On the basis of these assumptions, the IS phantom was sandwiched between 2- and 18-cm acrylic plates. The images were obtained with the LE collimator, with the energy window centered at 141 keV (±5%), and with or without a lead shield for 250 s of data acquisition. As in clinical practice with an LE collimator and a lead shield (lead shielding method), we used a lead shield that was 4 cm in diameter and 3 mm thick. A lead shield was placed directly on the phantom. The distance between the surface of the collimator and the lead shield was 1 cm.

Next, we studied the effects of the collimators and the energy window on image quality by imaging the CB phantom with an LEHR collimator or an ME collimator and the 2 energy windows centered at 141 and 146 keV (±5%). On this occasion, we excluded the evaluation of 146 keV for the LEHR collimator because that value lengthened the data acquisition time for the LEHR collimator as a result of the lower sensitivity of the LEHR collimator than of the ME collimator. The sensitivity of the ME collimator with the energy window centered at 146 keV (ME method) was equal to that of the lead shielding method.

Finally, we also investigated the usefulness of an ME collimator in patients with breast cancer. At 4 h after the peritumoral injection of 40 MBq (1.5 mL) of ^{99m}Tc-tin colloid, an anterior image was obtained for 250 s in the supine position by use of the FORTE camera attached to an LEHR collimator or an ME collimator.

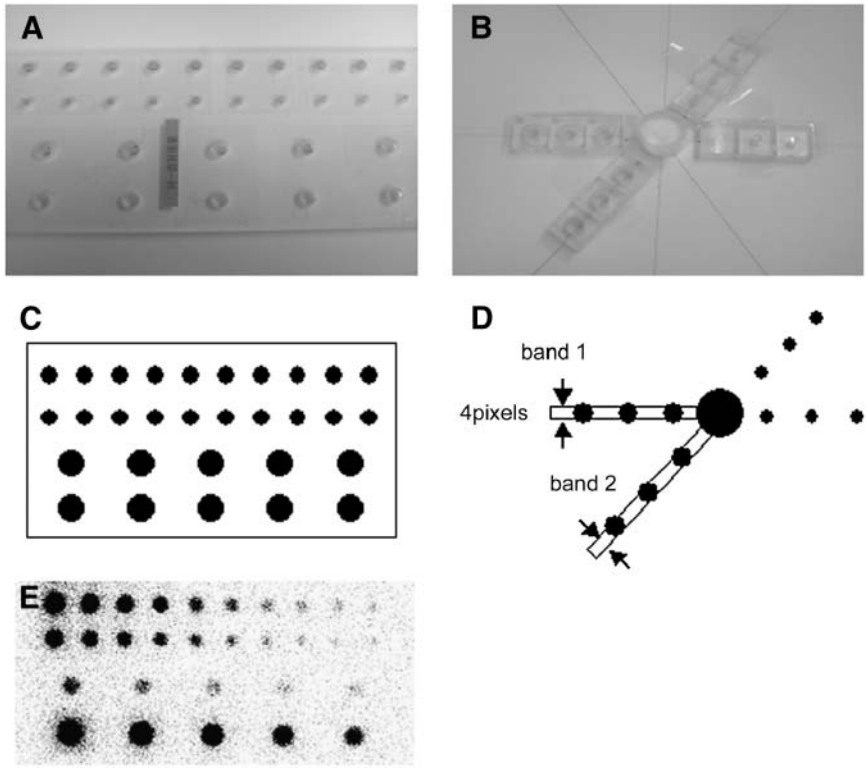

FIGURE 1. (A and C) Appearance and illustration of LN phantom, respectively. Holes were 8.5 mm (top row), 6.0 mm (middle row), and 12.0 mm (bottom rows) in diameter. Concentration of ^{99m}Tc-pertechnetate in 10 holes with same diameters was changed from 0.78 (right) to 400 kBq (left) per 200 μL in 1:2 increments over 10 steps. (B and D) Appearance and illustration of CB phantom, respectively. Holes containing radioactivity simulating lymph node were placed at 3, 5, and 7 cm from center of cylindric source. Band 1 and band 2 show regions for which profile curves were obtained in H and S directions, respectively. (E) Image of LN phantom taken with LEHR collimator and energy window centered at 141 keV. Note that sizes of hot spots changed with concentration of radioactivity.

Profile Curves

Profile curves were drawn by plotting continuously the counts in the regions of interest (ROIs) against the distance. As shown in Figure 1D, the size of each ROI on the CB phantom image was 1 pixel (2.36 mm) in length and 4 pixels (9.4 mm) in width. Counts were measured in the H and S directions, starting from the center of the injection site on the CB phantom image.

Evaluation of Image Contrast

Both the IS phantom and the LN phantom were used to determine contrast. The IS phantom was used to determine the background by placing ROIs of 4×4 pixels in 1-cm increments at 2–7 cm from the center of the injection site. Corresponding ROIs were placed on the LN phantom. Under such circumstances, 8.5-mm holes in the LN phantom were filled with 25, 100, and 400 kBq of the tracer. Contrast then was calculated with the following equation:

$$C = (SLN - BG)/(SLN + BG), \qquad \text{Eq. 1}$$

where C represents contrast, SLN represents the mean counts in the lymph node ROIs, and BG represents the background counts in the IS regions. Because we cannot discriminate the true counts included in the SLN from the BG counts, we used the BG counts obtained from the IS regions and assumed that the BG counts in the LN regions are equal to the values in the IS regions.

Using the values obtained for contrast, we evaluated the effects of lymph node site on image quality and appropriate acquisition time. To obtain the values for contrast at different data acquisition times, each IS phantom and each LN phantom were imaged for 1–15 min at 1-min intervals. On the basis of the values obtained from these images and Equation 1, the relationship between contrast and data acquisition times was obtained, and the most suitable time was selected.

RESULTS

Comparison of Images

Figure 1E shows an LN phantom image obtained with the LEHR collimator and the energy window centered at 141 keV. It is noteworthy that the sizes of hot spots decreased with a decrease in the concentration of radioactivity in the lymph nodes. As shown in Figure 2, the IS phantom image obtained with the FORTE camera and the LEHR collimator clearly was superior to that obtained with the DSX rectangular camera because the DSX rectangular camera with a GAP2 collimator and with or without a lead shield yielded prominent star-shaped artifacts.

The CB phantom image obtained with the ME collimator and the energy window centered at 141 keV showed a larger area of intense radioactivity and an increase in the surrounding background relative to the results obtained with the lead shielding method (Fig. 3). However, when the center of the energy window was shifted from 141 to 146 keV with the same ME collimator, the image showed a smaller area of intense radioactivity and a decrease in the background. Generally, the DSX rectangular camera yielded more star-shaped artifacts and a higher background around the area of intense radioactivity than did the FORTE camera.

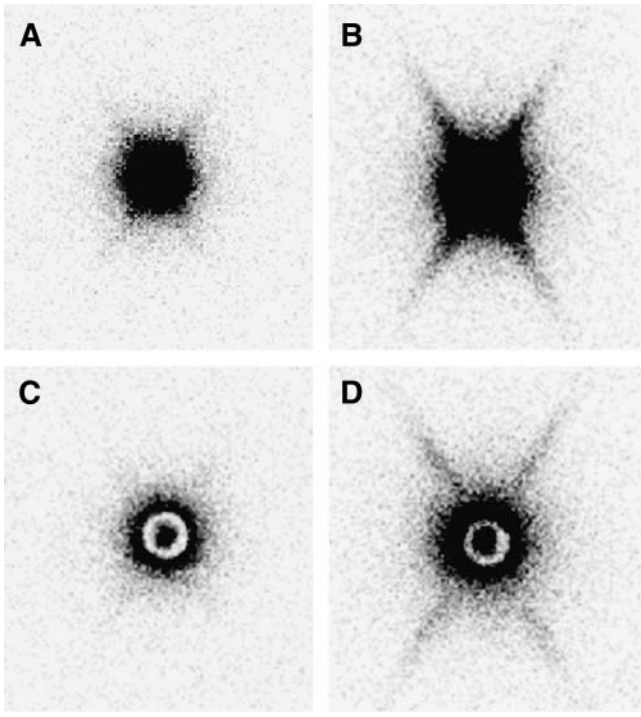

FIGURE 2. Comparison of IS phantom images obtained with 2 cameras. (A) FORTE camera without lead shield. (B) DSX rectangular camera without lead shield. (C) FORTE camera with lead shield. (D) DSX rectangular camera with lead shield. Images were taken with LE collimator and energy window centered at 141 keV (±5%) for 250 s of data acquisition. Prominent star-shaped artifacts are shown on DSX rectangular camera images.

Figure 4 shows static sentinel node lymphoscintigraphy (anterior views) in a patient with breast cancer. The star-shaped artifact was not completely eliminated with the lead shielding method. Therefore, there is a possibility of producing a study with false-negative results when the lead

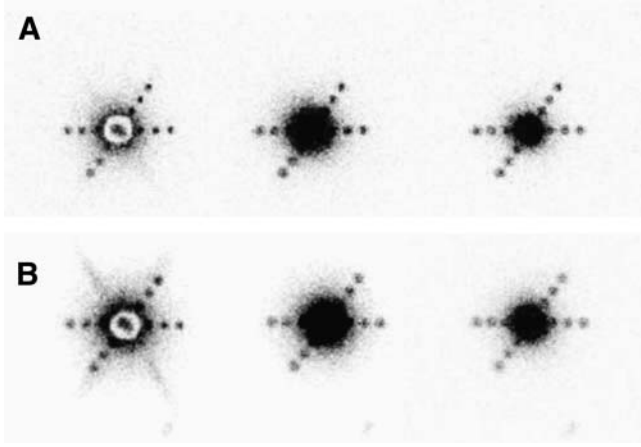

FIGURE 3. Comparison of CB phantom images obtained with FORTE camera (A) and DSX rectangular camera (B). (Left) 141 keV with LE collimator and lead shield—central white area shows effect of lead shield. (Middle) 141 keV with ME collimator. (Right) 146 keV with ME collimator.

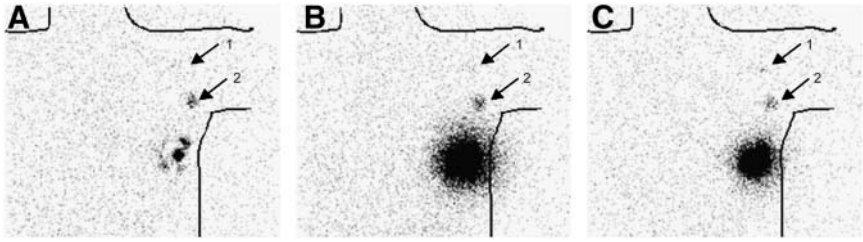

FIGURE 4. Static sentinel node lymphoscintigraphy (anterior views) in patient with breast cancer. (A) Image obtained with LEHR collimator and lead shield (lead shielding method). Lead shield covers imperfectly radioactivity at injection site. (B) Image obtained with ME collimator and energy window centered at 141 keV. (C) Image obtained with ME collimator and energy window centered at 146 keV (ME method). Arrows 1 and 2 show SLNs. ME method produced clear depiction of even small SLN (arrow 1).

shield does not cover the injection site. Even small SLNs could be depicted more clearly when the ME method was used than when an ME collimator with an energy window centered at 141 keV was used.

Evaluation of Profile Curves

Figure 5 shows the profile curves acquired with the FORTE and the DSX rectangular cameras. There was a marked difference in counts detected between the γ-cameras. The latter yielded higher counts than the former, indicating the greater sensitivity of the latter. The counts in the hot spots (lymph nodes) at 5 cm were higher than the values at 7 cm and lower than the values at 3 cm, reflecting the amount of scattering caused by the area of high radioactivity at the injection site. For the FORTE camera, similar curves were obtained with the lead shielding method and the ME method, except at 2 cm, at which the former yielded lower counts because of the lead shield. Furthermore, there was no observed difference between the H and the S directions with the ME method. (Therefore, we omit the distinction between the H and the S directions in the ME method.) Similar results were obtained with the 5-mm holes.

Evaluation of Image Contrast

As shown in Figure 6, contrast was greatly affected by the radioactivity in the lymph nodes. Contrast increased with increasing distance with radioactivity at 25 kBq, whereas contrast attained a plateau with increasing distance with radioactivity at 400 kBq. There was not such a marked difference between the H-direction data and the S-direction data. Contrast at 2 cm was lower with the ME method than with the lead shielding method. However, contrast at more than 3 cm was higher with the ME method than with the lead shielding method. Contrast attained a value of 1.0 (i.e., zero count for the background) at more than 5 and 7 cm with the ME method and the lead shielding method, respectively.

Figure 7 shows the relationship between data acquisition time and image contrast at 3 and 5 cm from the injection site. At 3 cm (Figs. 7A and 7B), similar trends were observed between the lead shielding method and the ME method. However, at 5 cm (Figs. 7C and 7D), a difference was observed between the methods. The ME method yielded higher contrast than the lead shielding method, even for the low level of radioactivity of 25 kBq, and contrast became stable after 5 min. Thus, the use of the ME method is expected to shorten the imaging time.

DISCUSSION

Phantoms

We made 3 types of phantoms based on the clinical data obtained from 25 breast cancer patients in our hospital. The

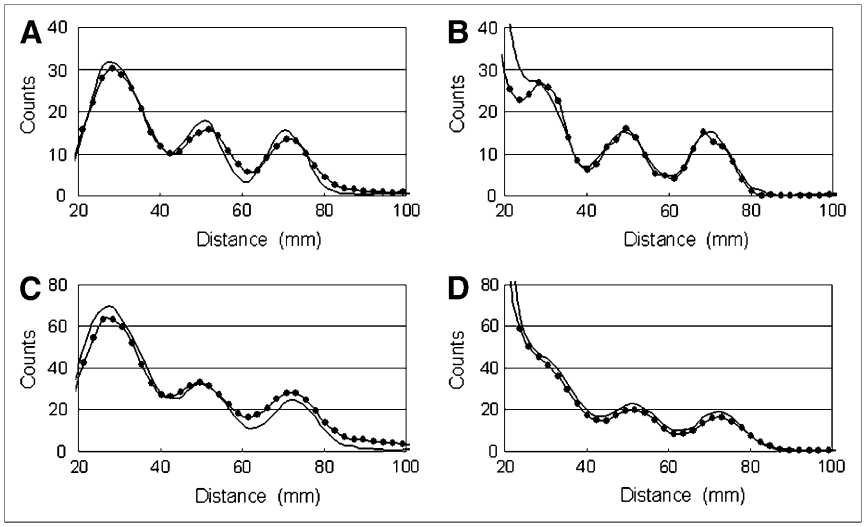

FIGURE 5. Profile curves acquired with 10-mm holes in CB phantom. (A and B) FORTE camera curves. (C and D) DSX rectangular camera curves. (A and C) Lead shielding method. (B and D) ME method. Note difference in longitudinal scales between FORTE and DSX rectangular camera graphs. Data obtained in H direction and data obtained in S direction are shown by plain solid line and by solid line with circles, respectively.

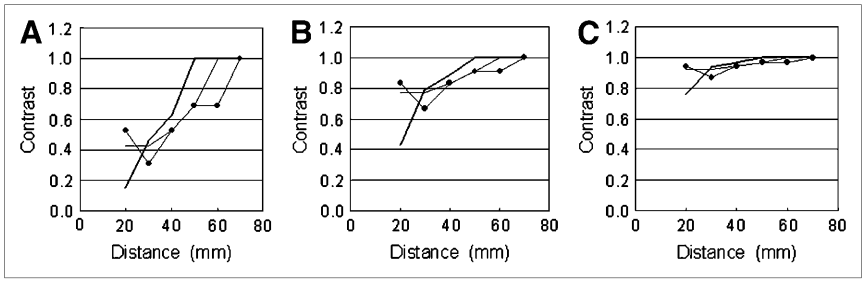

FIGURE 6. Relationship between lymph node site (distance from injection site) and image contrast with various levels of radioactivity for 5 min of data acquisition. (A) 25 kBq. (B) 100 kBq. (C) 400 kBq. Data obtained in H-direction with lead shielding method, data obtained in S-direction with lead shielding method, and data obtained with ME method are represented by plain thin line, by thin line with circles, and by thick line, respectively.

sizes of surgically excised SLNs ranged from 5 to 15 mm in diameter. The radioactivity in the SLNs corresponded to 2 kBq–1.2 MBq, representing less than 3% of the total dose of 40 MBq. These values were determined with the regression equation for counts and radioactivities estimated previously from LN phantoms (8.5-mm holes in Fig. 1C): $y = 0.1162x$ ($R^2 = 0.998$, $P < 0.01$), where y represents counts (counts/pixel) and x represents the amount of radioactivity (kBq). De Cicco et al. (*6*) reported that about 1% of the injected dose is retained per node when the tracer is injected subdermally into patients with breast cancer, with much smaller amounts being retained (0.1% of the injected dose per node) when the tracer is injected into the peritumoral parenchyma. We also found that the distance from the injection site to the SLN was 3.2–14.7 cm (7.5 ± 2.7 [mean ± SD] cm) on the lymphoscintigraphy anterior view and 3.6–15.7 cm (10.1 ± 2.9 cm) on the oblique view and that every SLN was located more than 3 cm from the injection site.

Comparison of Images

Previously, we reported that star-shaped artifacts appeared symmetrically in certain oblique directions, depending greatly on penetration through collimators (*16*). For example, as shown in Figure 2, star-shaped artifacts occurred slightly on FORTE camera images, whereas marked artifacts were observed on DSX rectangular camera images. As shown in Figure 5, the DSX rectangular camera yielded higher counts than the FORTE camera, reflecting its 1.6-fold-greater sensitivity (the value of 1.6 [7.4/4.6] can be obtained from the sensitivities of 7.4 and 4.6 cpm/kBq when the LE collimator is used with the DSX rectangular and FORTE cameras, respectively). Generally, LE collimators cause variations in penetration, resulting in the occurrence of star-shaped artifacts. The manufacturers demonstrated that 5% penetration would be caused by 150-keV energy photons with the DSX rectangular camera and 173-keV energy photons with the FORTE camera despite the same septal thickness of 0.15 mm for the LE collimator. In contrast, the septal thicknesses for the ME collimator were 1.14 and 0.9 mm with the FORTE and DSX rectangular cameras, respectively. Consequently, the difference in septal thickness between the collimators with the FORTE camera was 7.6-fold (1.14/0.15). This finding suggested that the ME collimator might be useful for decreasing the septal penetration of γ-rays.

Mariani et al. (*8*) reported that scattering was a major problem in the detection of an SLN located close to the

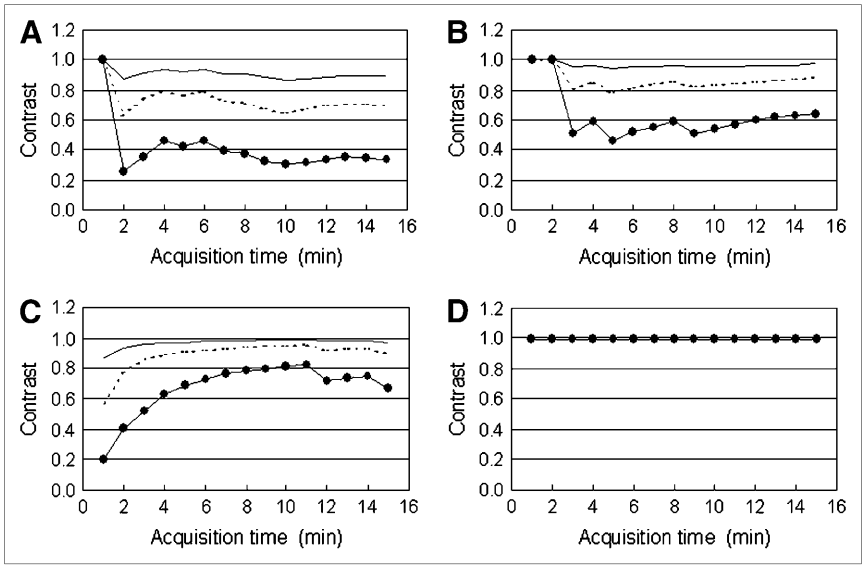

FIGURE 7. Relationship between image contrast and data acquisition time. (A) Contrast at 3 cm with lead shielding method. (B) Contrast at 3 cm with ME method. (C) Contrast at 5 cm with lead shielding method. (D) Contrast at 5 cm with ME method. Radioactivity concentrations of 400, 100, and 25 kBq/200 μL are represented by plain solid line, by dotted line, and by solid line with circles, respectively.

tumor. As star-shaped artifacts can impair the visualization of nearby SLNs, it is desirable that they will be decreased as much as possible. In the present study, the images obtained with the ME collimator and the energy window centered at 141 keV showed a greater increase in the background than did those obtained with the LE collimator because of greater scattering. However, when the center of the energy window was shifted upward by 5 keV, improved images with less background were obtained. Krynyckyi et al. (*13*) noted that excluding the lower energy window that is contaminated with scattering information will generally improve the quality of images. As reported by Glass et al. (*1*), scattering can be reduced by sampling only the high side of the photopeak, although doing so is achieved at the cost of camera field uniformity and counting rate. However, the degradation in uniformity with a digital γ-camera can be improved by correcting with a uniformity-corrected table in which the energy level is coincident with the off-center energy. Additionally, the decrease in counting rate can be diminished with an ME collimator with high sensitivity (*16*). In this respect, uniformity is of less concern in lymphoscintigraphy because the tracer is intensely concentrated in the lymphatics and at the injection site (*1*).

Lemstra et al. (*15*) performed a comparison between LE all-purpose (LEAP) and ME all-purpose (MEAP) collimators for SLN detection in breast cancer patients by phantom and clinical studies. In contrast to our results, they concluded that the LEAP collimator yielded better results than the MEAP collimator as a result of the better resolution and higher sensitivity. There were several differences between their study and our study. First, they used an LEAP collimator with a sensitivity 7% higher and a spatial resolution 30% higher than those of the MEAP collimator, whereas we used an ME collimator with a higher sensitivity but a lower spatial resolution than the LEHR collimator. With the FORTE camera, the sensitivity was improved by 1.35-fold from 4.6 cpm/kBq with the LEHR collimator to 6.2 cpm/kBq with the ME collimator, and the spatial resolution was degraded from 7.4 to 11.3 mm in full width at half maximum. With the DSX rectangular camera, the changes were not as great as with the FORTE camera. Second, they took no account of the differences in the energy window. Third, they did not note the direction of the star-shaped artifacts. Therefore, it is difficult to derive common conclusions from these 2 studies. They reported that the resolution advantage of the LEHR collimator over the LEAP collimator was theoretically minimal over short distances but that the lower sensitivity might lead to a preference for the LEAP collimator. The optimization for ^{99m}Tc of all LE collimators also causes star-shaped artifacts on LEHR collimator images. In contrast, Krynyckyi et al. (*17*) reported that a small amount of star-shaped artifacts could be eliminated by shifting the energy window upward for ^{99m}Tc.

One means of reducing star-shaped artifacts is to reduce the injection dose. However, this method is unfavorable because it results in a decrease in the amount of radioactivity that flows into the SLN and consequently decreases lymph node detection. Therefore, some authors recommend the use of a high-resolution collimator (*8*) or a super-high-resolution collimator (*7*).

Evaluation of Image Contrast

The ME method showed high contrast at a distance of more than 3 cm from the injection site. Because we confirmed from our clinical experience that the distance to the SLNs was more than 3 cm, these results are considered useful.

The results of the present study indicated that stable contrast could be obtained after 4 min for the ME method, indicating that 5 min would be sufficient in clinical use. The results indicated that the ME method has significant potential for shortening the acquisition time.

CONCLUSION

The first merit of the ME method is that there is no fear that the lymph node will be concealed by a lead shield. Moreover, improvement in the regional lymph node detection rate and shortening of the imaging time in breast cancer patients can be expected with a shift in the energy window.

ACKNOWLEDGMENTS

The authors thank M. Hatagawa, PhD, and all the radiological technologists at Osaka City University Hospital for technical support and N. Onoda, MD, T. Takashima, MD, and N. Motomura, MD, for valuable surgeons' comments. Finally, we are grateful to S. Shiomi, MD, and J. Kawabe, MD, nuclear medicine physicians, for advice.

REFERENCES

1. Glass EC, Essner R, Giuliano AE. Sentinel node localization in breast cancer. *Semin Nucl Med.* 1999;29:57–68.
2. Morton DL, Chan AD. The concept of sentinel node localization: how it started. *Semin Nucl Med.* 2000;30:4–10.
3. Alazraki NP, Styblo T, Grant SF, Cohen S, Larsen T, Aarsvold JN. Sentinel node staging of early breast cancer using lymphoscintigraphy and the intraoperative gamma-detecting probe. *Semin Nucl Med.* 2000;30:56–64.
4. Williams BS, Hinkle GH, Douthit RA, Fry JP, Pozderac RV, Olsen JO. Lymphoscintigraphy and intraoperative lymphatic mapping of sentinel lymph nodes in melanoma patients. *J Nucl Med Technol.* 1999;27:309–317.
5. Tanis PJ, Valdes Olmos RA, Muller SH, Nieweg OE. Lymphatic mapping in patients with breast carcinoma: reproducibility of lymphoscintigraphic results. *Radiology.* 2003;228:546–551.
6. De Cicco C, Cremonesi M, Luini A, et al. Lymphoscintigraphy and radioguided biopsy of the sentinel axillary node in breast cancer. *J Nucl Med.* 1998;39: 2080–2084.
7. Nieweg OE, Tanis PJ, Rutgers EJT. Summary of the second international sentinel node conference. *Eur J Nucl Med.* 2001;28:646–649.
8. Mariani G, Moresco L, Viale G, et al. Radioguided sentinel lymph node biopsy in breast cancer surgery. *J Nucl Med.* 2001;42:1198–1215.
9. Ellis RL, Seifert PJ, Neal CE, et al. Periareolar injection for localization of sentinel nodes in breast cancer patients. *Breast J.* 2004;10:94–100.
10. Koizumi M, Nomura E, Yamada Y, et al. Improved detection of axillary hot nodes in lymphoscintigraphy in breast cancer located in the upper lateral quadrant with additional projection imaging. *Ann Nucl Med.* 2004;18:707–710.

11. Dunnwald LK, Mankoff DA, Byrd DR, et al. Technical aspects of sentinel node lymphoscintigraphy for breast cancer. *J Nucl Med Technol.* 1999;27:106–111.
12. Feenstra C, Lansbergen SM, Buseman-Sokole E, Sloof GW. Imaging of sentinel nodes comparing different collimators [abstract]. *Eur J Nucl Med.* 2000;27:1006.
13. Krynyckyi BR, Miner M, Ragonese JM, Firestone M, Kim CK, Machac J. Technical aspects of performing lymphoscintigraphy: optimization of methods used to obtain images. *Clin Nucl Med.* 2000;25:978–985.
14. Haigh PI, Hansen NM, Giuliano AE, Edwards GK, Ye W, Glass EC. Factors affecting sentinel node localization during preoperative breast lymphoscintigraphy. *J Nucl Med.* 2000;41:1682–1688.
15. Lemstra C, Broersma M, Poot L, et al. Sentinel node detection in patients with breast cancer: low-energy all-purpose collimator or medium-energy collimator? *Clin Nucl Med.* 2004;29:609–613.
16. Tsushima H, Yamanaga T, Shimonishi Y, Ochi H. Usefulness of imaging method without using lead plate for sentinel lymph node scintigraphy [in Japanese]. *Kaku Igaku.* 2002;39:161–169.
17. Krynyckyi BR, Sata S, Zolty I, Kim DW, Kim SC, Knesaurek K. Sentinel node detection in patients with breast cancer: low-energy all-purpose collimator or medium-energy collimator? *Clin Nucl Med.* 2005;30: 369–370.